A Novel Method for High-Resolution Characterization of Vein Deformation Under Arterial Blood Pressure

Yan-Ting Shiu[1], Arnold David Gomez[1], Brian Watson[1], Huan Li[1], Ilya Zhuplatov[1], Alfred Cheung[1,2], Edward Hsu[1]

[1]U of Utah, SLC, UT, USA
[2]VASLCHCS, SLC, UT, USA

Introduction

Arteriovenous fistulas (AVF) often fail to mature, likely due to aberrant hemodynamic stress-induced wall strain. To assess the influence of pressure-induced wall strain on AVF maturation, it is important to have a better understanding of vein mechanics. Measuring the strain of thin venous walls is challenging because changes in length are often less than 100 µm, which is below the resolution for MRI or conventional ultrasound. Here, we present a strain analysis method based on micro-computer tomography (µCT) to characterize deformation of thin vein samples under pressure with the following features:

- *Morphological depiction at 17 µm resolution, and*
- *Characterization of local 3D strain tensor.*

Methods

Contrast Optimization

To determine the contrast needed for imaging soft tissues [1], sections of a vein sample were treated in an isotonic solution of Lugol's Iodine at different concentrations and for different lengths of time.

Testing Apparatus

A µCT-compatible, hydrostatic pressure loading testing apparatus (Fig. 1) was built to pressurize a freshly excised abdominal porcine vein (unloaded, and under 30 mmHg) while imaging at 17-micron resolution.

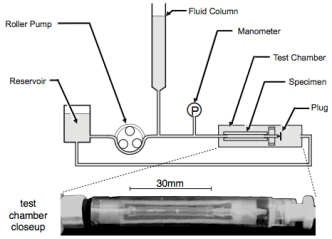

Figure 1. Testing Chamber: The vein specimen is placed inside a chamber, where it is kept pressurized at 0 or 30 mmHg while being imaged via mCT.

Measuring Strain via Registration with Hyperelastic Warping

The volumetric images acquired at 0 mmHg were manually segmented and meshed (Fig. 2), and used as the template for Hyperelastic Warping. Imagery acquired at 30 mmHg served as target. Two strain measurements were obtained, assuming Veronda-Westmann material coefficients from the saphenous vein [2] and coronary sinus [3], respectively.

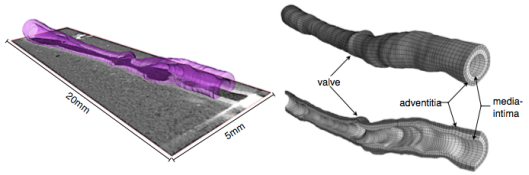

Figure 2. Finite Element Geometry: The segmented images acquired at 0 mmHg (left) were used to construct a finite-element mesh (right), capturing detailed anatomical features like vessel layers and a valve.

Results and Discussion

Image-Driven Deformation to Measure Strain

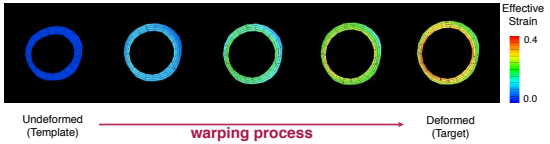

Figure 3. Image-Driven Deformation: Progression of a radial cross-section of vein specimen during deformation based on unloaded (Template) and loaded (Target) specimen imagery; the color represents effective strain.

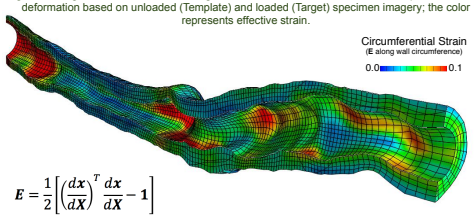

$$E = \frac{1}{2}\left[\left(\frac{dx}{dX}\right)^T \frac{dx}{dX} - 1\right]$$

Figure 4. Local Strain Measurement: Longitudinal cross-section of specimen where the colors represent the Green-Lagrange Strain tensor (**E**) projected in the circumferential direction. In the equation: X and x stand for reference and current coordinates, respectively, and **1** represents the Kronecker delta.

Fig. 3 shows the image-driven deformation process starting on the undeformed configuration, which matches the template image, and ending on the deformed configuration, which conforms to the target image. In Hyperelastic Warping, the images produce body forces, which deform a finite element mesh assuming a material model [4]. Fig. 4 shows highly localized deformation in the circumferential direction which, following the theoretical expectation, depends on wall thickness. Additional directions of principal strains followed similar trends.

Image-Driven Deformation Unaffected by Material Coefficients

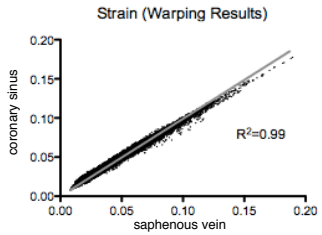

Figure 5. Strain Results Comparison: The scatter plot shows elemental values for the second principal strain (circumferential direction).

Fig. 5 shows that circumferential strain results obtained using both sets of material coefficients were nearly identical (also true with the other principal components of the strain tensor). The consistency of results indicate that strain measurements via Hyperelastic Warping only depend on imagery changes, and not on other registration-related or computational factors.

Contrast Agent Selection

Fig. 6 shows µCT images of vein sections after different Iodine treatments. In this application, the best tissue contrast was obtained using 10% Lugol solution and a 3-hour soaking duration. Visual inspection suggested insignificant shrinking. Therefore, vessel sample geometry can be reconstructed with minimum constitutive changes, although the exact impact of the treatment has yet to be quantified.

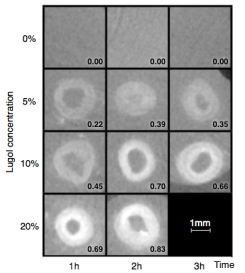

Figure 6. Contrast After Different Treatment Strategies: The mCT Images of sections from the same vein had various levels of contrast (numbers in black).

Furthermore, the iodine treatment resulted in stable contrast during imaging, which provided data with sufficient quality for segmentation and image registration.

Conclusion

We have developed a robust protocol to assess the strain of thin vein samples under pressure. The three-dimensional finite strain tensor was defined across the entire vein's geometry, which contained complex anatomical features including non-uniform wall thickness, valves, and bifurcations. Further serial analyses in larger studies will illuminate the relationship between early wall strain and subsequent AVF maturation, laying foundations to devise strategies for promoting AVF maturation.

This method shows significant promise for regional tissue characterization across a number of geometries and conditions, with the ability to measure three-dimensional regional strain in vessels whose lumen diameter is of the order of 1 mm and detailed anatomical features of the order of 100 µm.

Acknowledgements

- Musculoskeletal Research Laboratories (U of U) for providing Hyperelastic Warping implementation
- Special Thanks to David Zou (U of U) for image segmentation
- NIH Funding through grant R01-DK088777

References

1. Degenhart K, et al. Circ Cardiovasc Imaging. 2010, 3:314-22.
2. Gusic RJ, et al. J Biomech. 2005, 38:1770-9.
3. Pahm T, et al. J Mech Behav Biomed Mater. 2012, 6:21-9.
4. Rabbitt RD, et al. Proc SPIE (Vision Geometry IV). 1995, 2573:252-265.